Artificial neural network as a predictive tool for emissions from heavy-duty diesel vehicles in Southern California

N Hashemi and N. N. Clark

International Journal of Engine Research 2007 8: 321
DOI: 10.1243/14680874JER00807

Artificial neural network as a predictive tool for emissions from heavy-duty diesel vehicles in Southern California

N Hashemi[1]* and **N N Clark**[2]
[1]Department of Mechanical Engineering, Virginia Polytechnic Institute and State University, Blacksburg, Virginia, USA
[2]Department of Mechanical and Aerospace Engineering, West Virginia University, Morgantown, West Virginia, USA

The manuscript was accepted after revision for publication on 7 April 2007.

DOI: 10.1243/14680874JER00807

Abstract: An artificial neural network (ANN) was trained on chassis dynamometer data and used to predict the oxides of nitrogen (NO_x), carbon dioxide (CO_2), hydrocarbons (HC), and carbon monoxide (CO) emitted from heavy-duty diesel vehicles. Axle speed, torque, their derivatives in different time steps, and two novel variables that defined speed variability over 150 seconds were defined as the inputs for the ANN. The novel variables were used to assist in predicting off-cycle emissions. Each species was considered individually as an output of the ANN. The ANN was trained on the Highway cycle and applied to the City/Suburban Heavy Vehicle Route (CSHVR) and Urban Dynamometer Driving Schedule (UDDS) with four different sets of inputs to predict the emissions for these vehicles. The research showed acceptable prediction results for the ANN, even for the one trained with only eight inputs of speed, torque, their first and second derivatives at one second, and two variables related to the speed pattern over the last 150 seconds. However, off-cycle operation (leading to high NO_x emissions) was still difficult to model. The results showed an average accuracy of 0.97 for CO_2, 0.89 for NO_x, 0.70 for CO, and 0.48 for HC over the course of the CSHVR, Highway, and UDDS.

Keywords: artificial neural networks, emissions, heavy duty diesel vehicles, off-cycle, NO_x, smooth speed pattern

1 INTRODUCTION

The United States Environmental Protection Agency (EPA) defines the National Ambient Air Quality Standards (NAAQS) and also sets emissions standards for heavy-duty diesel engines. Diesel engines are extensively used to power heavy-duty on-road vehicles and also non-road equipment as a result of their outstanding fuel economy. Oxides of nitrogen (NO_x), particulate matter (PM), hydrocarbons (HC), and carbon monoxide (CO) are the main contributions of on-road heavy-duty diesel vehicles to the atmospheric inventory. NO_x reacts with HC and sunlight to form ground-level ozone and also plays an important role in fine particulate matter formation [**1**]. The EPA estimates that 27 per cent of on-road vehicle emissions of NO_x and more than 60 per cent of PM are contributed by heavy-duty vehicles throughout the nation, although these heavy-duty vehicles are only 2 per cent of the total on-road fleets [**2**]. For the development of an emissions inventory, it is necessary to have a database of the emissions data, also known as the base year inventory [**3**]. To satisfy the need for improved analysis that does not rely simply on engine standards, the EPA's Office of Transportation and Air Quality (OTAQ) is working on a new system defined as the multi-scale motor vehicles and equipment emission system (MOVES) [**4**]. The MOVES model estimates emissions for on-road and non-road sources, covering a wide range of pollutants [**5**] and makes use of the concept of vehicle specific power. It is possible to perform analysis over a range of

* *Corresponding author: Department of Mechanical Engineering, Virginia Polytechnic Institute and State University, Blacksburg, VA 24061, USA. email: nastaran@vt.edu*

scales, from road planning analysis to national inventory estimation with a MOVES philosophy. There are also other approaches to inventory prediction. For instance, Kern *et al.* [**6**] have utilized emissions factors based on instantaneous engine power, vehicle power, vehicle speed, and acceleration.

This paper has the objective of developing a predictive tool for heavy-duty vehicle emissions, without resorting to a vehicle model and engine emissions data. The paper explores the use of artificial neural networks (ANNs) for this purpose. Most previous ANN diesel engine emissions modelling has used engine-based data. Clark *et al.* [**7**] trained an ANN using engine speed and torque to predict NO_x and CO_2 from vehicles in conjunction with a powertrain simulator for conventional and hybrid electric vehicles. Krinjnsen *et al.* [**8**] showed that the ANN was an accurate method to predict NO_x emissions and could be used in selective catalytic reduction (SCR) applications. Yuanwang *et al.* [**9**] used the cetane number to predict the exhaust emissions from an engine using an ANN. Fuel composition parameters along with engine torque and speed were used by De Lucas *et al.* [**10**] to predict particulate emissions with an ANN, and several other papers have reported the training of an ANN on diesel engine data alone.

2 VEHICLE DATA

This ANN modelling used NO_x, HC, CO, and CO_2 data that were measured from vehicles operating in Southern California, as part of the Gasoline/Diesel PM Split Study, which was performed to gather emissions data from both light-duty [**11**, **12**] and heavy-duty [**13**] vehicles. This study 'was conducted to quantify the relative contributions of tailpipe emissions from gasoline-powered motor vehicles and diesel-powered motor vehicles to the ambient concentrations of fine particulate matter (PM 2.5) in the urbanized region of Southern California using an organic compound-based chemical mass balance model (CMB)' [**14**], and the context for this study is presented in reference [**15**]. The heavy-duty diesel vehicle component of this study was undertaken using the West Virginia University Transportable Heavy-Duty Vehicle Emissions Testing Laboratories [**13**]. Trucks and buses were driven through transient speed–time cycles on a chassis dynamometer, with inertial load provided by sets of flywheels. Wind drag and tyre rolling losses were mimicked using eddy-current power absorbers. Emissions data were recorded using an exhaust dilution tunnel and research grade emissions analysers. Hydrocarbons were measured using a flame ionization detector, carbon monoxide and dioxide were measured using infrared absorption, and oxides of nitrogen were measured using chemiluminescence. PM was measured on a cycle-averaged basis using filters. The heavy-duty vehicles in the study included 16 trucks with a gross vehicle weight (GVW) over 33 000 lb. The City/Suburban Heavy Vehicle Route (CSHVR) [**16**] and the Highway cycle [**13**] were employed, and several vehicles were tested using the Urban Dynamometer Driving Schedule (UDDS) from the US Code of Federal Regulations. The CSHVR represents urban transient truck operation, while the Highway cycle emphasizes freeway operation. The UDDS contains both freeway and non-freeway activity. Continuous data gathered during this study were used in the present ANN research, but the ANN modelling was not a specific objective of the Gasoline/Diesel PM Split Study.

3 DATA DESCRIPTION

From the existing database, a group of vehicles in the 33 000–80 000 lb weight range was selected. There were six tractor trucks in this group and their characteristics are listed in Table 1. Vehicles 1 and 2 were exercised through three different driving test schedules, the City/Suburban Heavy Vehicle Route (CSHVR), Highway cycle, and Heavy-Duty Urban Dynamometer Driving Schedule (UDDS or Test D) [**16**]. Vehicles 3 to 6 were exercised only through the CSHVR and Highway cycle.

Table 1 Vehicle and engine descriptions

Vehicle	Type	Year	Manufacturer	Odometer mileage	GVW (lb)	Vehicle tested weight (lb)	Engine	Displacement (litre)
Vehicle 1	Tractor truck	1985	Freightliner	769 413	80 000	42 000	Caterpillar 3406B	14.6
Vehicle 2	Tractor truck	1994	Freightliner	639 105	80 000	42 000	Detroit diesel series 60	12.7
Vehicle 3	Tractor truck	1998	Sterling	327 300	80 000	42 000	Detroit diesel series 60	12.7
Vehicle 4	Tractor truck	1999	Sterling	272 307	80 000	42 000	Caterpillar C-12	12
Vehicle 5	Tractor truck	2000	Sterling	255 880	80 000	42 000	Caterpillar C-12	12
Vehicle 6	Tractor truck	2001	Volvo	327 300	80 000	42 000	Cummins N14-370	14

4 POWER DISPERSION MODELLING

To measure the emissions, a standard full-scale dilution tunnel and emissions analysers were employed. When the exhaust gas passes through the dilution, sampling, and measurement system, gas elements take different routes through the dilution tunnel and sampling lines [**17**]. This phenomenon is called axial dispersion and is superimposed on the time delay associated with transport through the system. In addition, the response behaviour of the analyser also contributes to this delay and this time dispersion. In order to find the time delay between the actual emission production instance and emissions measuring time, vehicle power and the emissions data series were cross-correlated (see Appendix 2) and the time delay correction for a maximum product was sought. Power was selected as a reference due to the relationship of this parameter to engine emissions [**18**]. The average shifting time was 8–9 seconds for NO_x, 12–14 seconds for CO, and 13–15 seconds for CO_2. The HC shifting time was variable for different cycles. HC time alignment can be difficult because HC may not increase monotonically with power.

The axial dispersion of the emissions species is important to consider because otherwise the emissions data used to train the ANN do not correspond correctly to the speed and torque data because the speed and torque data do not experience significant dispersion during measurement. Considering the known relationship between the power and emissions, Clark *et al.* [**19**] applied a dispersion model to the axle power to find the emissions dispersion model. They assumed that if the power were artificially dispersed in the same way that the emissions data were dispersed by the sampling and measurement system, then measured emissions and dispersed power would correlate well. Jarrett [**20**] added two variables of a and b to the Levenspiel equation. However, in his model the discretized dispersion function did not sum to unity and its associated error was about 4 per cent. Baskaran and Clark [**21**], by using data from injecting CO_2 into a dilution tunnel for a period of 4 seconds, showed that the analyser response had delay and diffusion. Their dispersion and delay model included a starting dead time and a gamma distribution that represented the response of well-mixed tanks in series. Their values of C_i (which represented the second-by-second responses to a unit pulse input) were normalized in their model. In this research, to achieve the best power dispersion model, a linear correlation between the dispersed power and measured CO_2 was used. The vessel dispersion number (VDN) [**22**], a dimensionless group characterizing the dispersion in the tunnel, sampling lines, and analysers, was varied until an optimum correlation was found. The VDN was represented by $D/(UL)$, where D is the dispersion coefficient and U is average velocity of the fluid in a pipe of length L. In most cases, the cross-correlation of power and CO_2 estimated the time delay at 15 seconds. Therefore the centroid of the distribution was assumed to be located at 15 seconds. Values of t_i were defined over a period of 31 seconds to show the absolute nature of delay, which consisted of onset time and dispersion time (Fig. 1). Table 2 shows the values of $C_i \in [1, 31]$ corresponding to t_i and normalized to 1. Table 2 should be interpreted in the following way: if the emissions are zero except that a unit pulse emissions input occurs at time zero, the analyser reports almost no emissions for 8 seconds, followed by a distribution in time. For example, the emissions value is about 0.023 at 11 seconds after the pulse, and about 0.118 at 17 seconds after the pulse.

Power was dispersed for different values of $D/(UL)$, and CO_2 versus dispersed power was mapped to find the best dispersion model. Tables 3 to 5 show the R^2 values of the linear fits ($D/(UL)$ values equal to 0.085,

Table 2 Normalized C_i values relevant to $t_i \in [1, 31]$

C_1	7.4 E-130	C_{12}	6.4 E-2	C_{23}	2.1 E-3
C_2	1.2 E-56	C_{13}	1.2 E-1	C_{24}	8.5 E-4
C_3	1.0 E-32	C_{14}	1.6 E-1	C_{25}	3.2 E-4
C_4	4.3 E-21	C_{15}	1.8 E-1	C_{26}	1.2 E-4
C_5	2.1 E-14	C_{16}	1.6 E-1	C_{27}	4.1 E-5
C_6	3.7 E-10	C_{17}	1.2 E-1	C_{28}	1.4 E-5
C_7	2.5 E-7	C_{18}	7.7 E-2	C_{29}	4.6 E-6
C_8	2.3 E-5	C_{19}	4.4 E-2	C_{30}	1.5 E-6
C_9	5.4 E-4	C_{20}	2.3 E-2	C_{31}	4.6 E-7
C_{10}	4.9 E-3	C_{21}	1.1 E-2		
C_{11}	2.3 E-2	C_{22}	5.1 E-3		

Table 3 R^2 results of linear fit for CO_2 versus dispersed power using CSHVR [**16**] data

	$D/(UL) = 0.085$	$D/(UL) = 0.02$	$D/(UL) = 0.011$
Vehicle 1	0.7956	0.8507	0.8507
Vehicle 2	0.7732	0.8552	0.8668
Vehicle 6	0.6640	0.8265	0.8684

Table 4 R^2 results of linear fit for CO_2 versus dispersed power using Highway cycle data

	$D/(UL) = 0.085$	$D/(UL) = 0.02$	$D/(UL) = 0.011$
Vehicle 1	0.8868	0.9262	0.9274
Vehicle 2	0.7885	0.8302	0.8131
Vehicle 6	0.8435	0.9002	0.9067

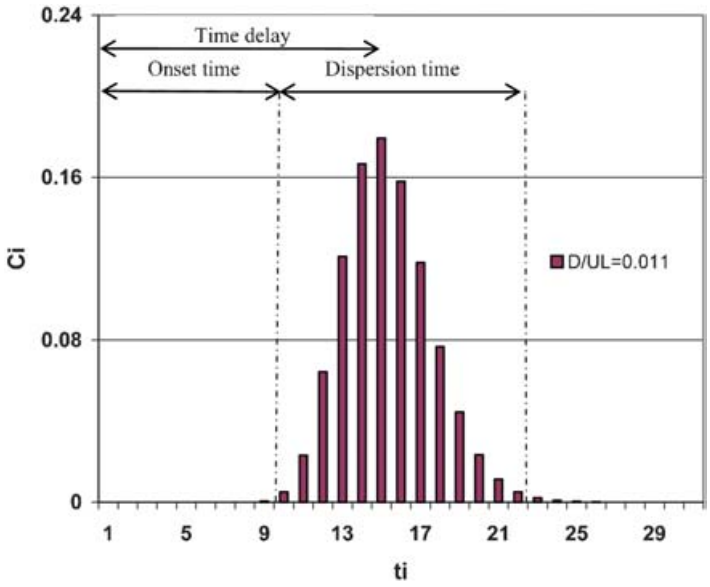

Fig. 1 Normalized C_i relevant to t_i over a 31 second period shows an onset time of 10 seconds and dispersion period of 13 seconds

Table 5 R^2 results of linear fit for CO_2 versus dispersed power using UDDS [**23**] data

	$D/(UL)=0.085$	$D/(UL)=0.02$	$D/(UL)=0.011$
Vehicle 1	0.8625	0.9040	0.9119
Vehicle 2	0.7848	0.8593	0.8908

0.02, and 0.011). $D/(UL)$ values greater than 0.085 and smaller than 0.011 yielded extremely poor fits. The best linear fit for $D/(UL)=0.011$ represented an onset time of 10 seconds and a dispersion time of 13 seconds. In this case, the dispersion curve (discretized as C_i values) followed the non-symmetric $D/(UL)>0.01$ curve (see equation (11) in Appendix 3), but it was close to a Gaussian symmetric curve. Figure 2 shows the continuous curves for different values of $D/(UL)$ versus θ. Neglecting $C_i<0.001$, $\theta \in [0.333, 2.067]$ for $D/(UL)=0.085$, which shows the 5 second onset time with a 26 second dispersion period. Similarly, $\theta \in [0.533, 1.800]$ for $D/(UL)=0.02$, which corresponds to an 8 second onset time and 19 second dispersion period. $\theta \in [0.667, 1.533]$ for

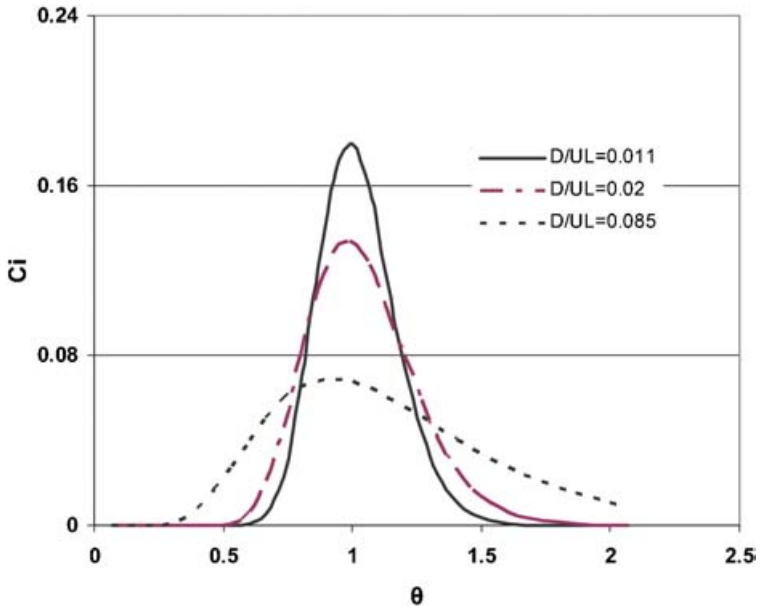

Fig. 2 Dispersion of the point injection for three different values of $D/(UL)$ (0.085, 0.02, 0.011) corresponding to equation (11)

$D/(UL) = 0.011$ was described above as the best power dispersion model. To confirm the precision of this model, the integral of the CO_2 over the cycle was compared to the integral of the dispersed CO_2 and the difference was only 0.01 per cent.

The instantaneous power was correlated with the vehicle emissions and then was dispersed using the non-symmetric dispersion model. The measured CO_2 was linearly mapped versus dispersed power. The results confirmed the relationship of the measured CO_2 and the dispersed power distinctly (Tables 3 to 5). Figure 3 shows the linear fit of $R^2 = 0.9067$ with the $D/(UL) = 0.011$ dispersion model for vehicle 6 exercised through the Highway cycle. This was the dispersion chosen for use in conjunction with the ANN modelling described below. Preprocessing of data in this way was essential before establishing ANN models to relate emissions to vehicle or engine behaviour.

5 ARTIFICIAL NEURAL NETWORKS

ANNs are non-mechanistic modelling techniques suitable for non-linear correlations. The ANNs are composed of simple elements operating in parallel and their function is dependent on the connections of elements. By adjusting the values of connections (weights), an ANN can be trained. The objective is to obtain a specific output from a particular input. The characteristic of elements and their connections determines the structure of the network. The learning algorithm determines the strength of the connections to be trained and obtains a desired output [**24**]. Standard backpropagation (BP) is a gradient descent algorithm in which the gradient is computed for non-linear multilayer networks. The trained BP network should yield reasonable results when new inputs are introduced to the network. Typically, a new input that is similar to the input on which the network has already been trained is introduced to the network and presents an output similar to the correct output for input vectors used in training. This property makes it possible to train a network on a specific set of input/target pairs and obtain good results without training the network on all possible input/output pairs [**25**]. The performance index for the BP algorithm and the least mean square (LMS) algorithm is identical [**26**] and defined as

$$\hat{F}(x) = [t(k) - a(k)]^2 = e^2(k) \tag{1}$$

where $a(k)$ is the output of the network, $t(k)$ is the correct output, and $e(k)$ is the error at iteration k. The steepest descent algorithm with a constant learning rate (α) for the performance index is

$$\mathbf{w}^m_{i,j}(k+1) = \mathbf{w}^m_{i,j}(k) - \alpha \frac{\partial \hat{F}}{\partial \mathbf{w}^m_{i,j}} \tag{2a}$$

$$\boldsymbol{b}^m_i(k+1) = \boldsymbol{b}^m_i(k) - \alpha \frac{\partial \hat{F}}{\partial \boldsymbol{b}^m_i} \tag{2b}$$

where $\mathbf{w}_{i,j}$ is a weight matrix and $\boldsymbol{b}_i$ is a bias vector. The input to layer m is a function of the weight and bias in that layer. Using the chain rule and defining the sensitivity (s^m_i) of $\hat{F}$ to changes in the ith input at layer m by the following equation

$$s^m_i = \frac{\partial \hat{F}}{\partial n^m_i} \tag{3a}$$

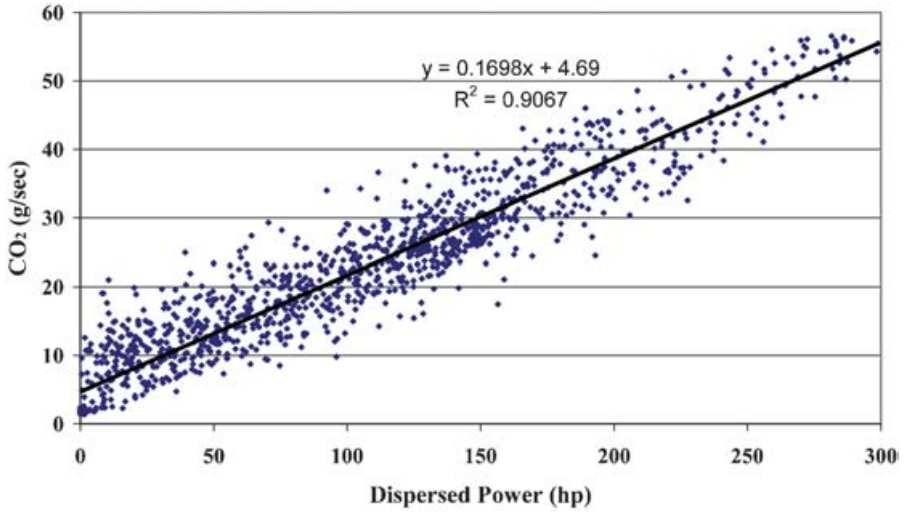

Fig. 3 Linear fit of CO_2 versus dispersed power with $D/(UL) = 0.011$ for vehicle 6 exercised through the Highway cycle [**16**]

where

$$n_i^m = \sum \mathbf{w}_{i,j}^m a_j^{m-1} + \boldsymbol{b}_i^m \tag{3b}$$

the BP algorithm can be expressed by

$$\mathbf{w}_{i,j}^m(k+1) = \mathbf{w}_{i,j}^m(k) - \alpha s_i^m a_j^{m-1} \tag{4a}$$

$$\boldsymbol{b}_i^m(k+1) = \boldsymbol{b}_i^m(k) - \alpha s_i^m \tag{4b}$$

The ANN used to predict the emissions was NeuroShell 2 release 4.0, created by Ward Systems Group. The BP network with various activation functions was selected. The hidden layer was discretized to three different parts with dissimilar transfer functions to identify different features in each pattern and to view the data in three different ways. For instance, the $f(x) = \exp(-x^2)$ fortified the middle range of the input while the $f(x) = 1 - \exp(-x^2)$ brought out meaningful characteristics in the extremes of the data. The number of inputs determined the number of neurons in the input layer. The numbers of neurons in the hidden layers were a function of input and output numbers and training patterns. Output neurons were equal to the outputs. Figure 4 shows the BP networks used in this research.

In this research, the ANN was trained individually for each emission species (NO_x, CO_2, CO, and HC) as the ANN output. Considering the known relationship [**28**, **29**] between the vehicle emissions and the power, two variables of hub rotational speed (which is proportional to vehicle speed) and axle torque were chosen as major inputs for training the ANN. The ANN was trained with three different sets of inputs (8, 14, and 20 inputs). The 20-input ANN consisted of the two variables of hub speed and torque and their first and second derivatives at three different time ranges (1, 5, and 10 seconds) in addition to two novel variables in speed defined as

$$\mathrm{Del}(t) = \mathrm{Spd}^2(t) - \overline{\mathrm{Spd}}^2(t) \tag{5}$$

$$\mathrm{Diff}(t) = \int_{t-t_l}^{t} [\mathrm{Spd}^2(t) - \overline{\mathrm{Spd}}^2(t)] \tag{6}$$

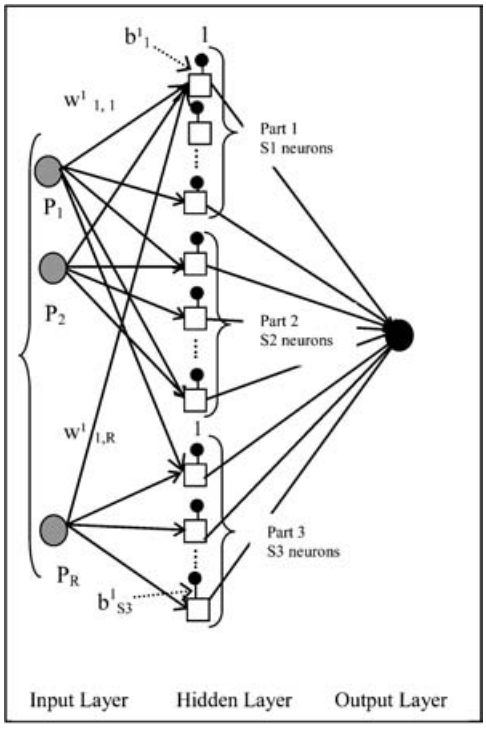

Fig. 4 Backpropagation ANN. This illustration combines information from *neural network design* [**26**] *NeuroShell2 users's manual* [**27**].

where

$$\overline{\mathrm{Spd}}(t) = \frac{\int_{t-t_l}^{t} \mathrm{Spd}(t)}{t - (t - t_l)}$$

Values of t_l were chosen to be equal to 50, 100, and 150 seconds in an effort to track 'off-cycle' emissions, which are described below. Table 6 shows the inputs used in the 20-input ANN. The 14-input ANN used inputs of the hub speed and torque and their first and second derivatives at three different time ranges (1, 5, and 10 seconds) and the ANN with 8 inputs used speed, torque, their first and second derivatives at 1 second and Diff(t) and Del(t) in 150 seconds as inputs.

Table 6 The S and T present dispersed speed and torque respectively; $\mathrm{d}S/\mathrm{d}t$ (1 s) shows the first derivative of dispersed speed over 1 second; $\mathrm{d}^2S/\mathrm{d}t^2$ (1 s) shows the second derivative of dispersed speed over 1 second; inputs 15, 16, and 17 refer to equation (5) and inputs 18, 19, and 20 refer to equation (6)

Input 1	Dispersed speed (S)	Input 11	$\mathrm{d}S/\mathrm{d}t$ (10s)
Input 2	Dispersed torque (T)	Input 12	$\mathrm{d}T/\mathrm{d}t$ (10s)
Input 3	$\mathrm{d}S/\mathrm{d}t$ (1 s)	Input 13	$\mathrm{d}^2S/\mathrm{d}t^2$ (10s)
Input 4	$\mathrm{d}T/\mathrm{d}t$ (1 s)	Input 14	$\mathrm{d}^2T/\mathrm{d}t^2$ (10s)
Input 5	$\mathrm{d}^2S/\mathrm{d}t^2$ (1 s)	Input 15	$S^2 - S^2_{\mathrm{avg}}$ (50s)
Input 6	$\mathrm{d}^2T/\mathrm{d}t^2$ (1 s)	Input 16	$S^2 - S^2_{\mathrm{avg}}$ (100s)
Input 7	$\mathrm{d}S/\mathrm{d}t$ (5 s)	Input 17	$S^2 - S^2_{\mathrm{avg}}$ (150s)
Input 8	$\mathrm{d}T/\mathrm{d}t$ (5 s)	Input 18	$\int [S^2 - S^2_{\mathrm{avg}}\ (50\ \mathrm{s})]$ over the last 50 s
Input 9	$\mathrm{d}^2S/\mathrm{d}t^2$ (5 s)	Input 19	$\int [S^2 - S^2_{\mathrm{avg}}\ (100\ \mathrm{s})]$ over the last 100 s
Input 10	$\mathrm{d}^2T/\mathrm{d}t^2$ (5 s)	Input 20	$\int [S^2 - S^2_{\mathrm{avg}}\ (150\ \mathrm{s})]$ over the last 150 s

The Diff(t) and Del(t) variables were chosen to improve the network prediction accuracy. These two functions serve to approximate the 'off-cycle' emissions behaviour exhibited by many engines manufactured in the 1990s. It was typical that after the vehicle had cruised for a short while (so that engine speed was not transient), an alternate injection timing strategy was invoked to improve fuel economy. The 'off-cycle' emissions are confusing to the ANN because they represent a second possible output for the same set of inputs. For instance, emissions of NO_x are strongly affected by injection timing changes while emissions of CO_2 are affected only slightly. This 'off-cycle' timing behaviour was curtailed following a consent decree between manufacturers and the US government [**30**]. Functions to detect steady behaviour (Diff(t) and Del(t)) offer the ANN a method for predicting timing changes, based on a duration of cruising behaviour, although these functions cannot hope to mimic all manufacturers' strategies faithfully.

6 RELATIVE CONTRIBUTION FACTORS

To show the effect of a particular input in ANN training, the relevance of each input in comparison to the other inputs was considered. Research was initiated with the 20-input ANN. The architecture of this ANN consisted of a hidden layer with three different activation functions. Each part in the hidden layer had 15 neurons and every input was connected to each neuron by a weight. The output layer was a one-neuron layer relevant to the desired emission species. In further steps, the number of inputs was decreased to those specific inputs that contributed more to the prediction results. The hidden layer of the 14-input ANN was composed of 14 neurons in each part. However, the 8-input ANN had 13 neurons in each part of the hidden layer. The results showed that the dispersed speed was the most controlling input in the ANN training for all the emissions prediction cases. This is understandable because speed on its own offers some measure of output power. The second derivative of torque, first derivatives of speed and torque, and the Diff(t) variable were the next most powerful inputs respectively. The torque itself might be expected to be an input with a strong input, but it is dissimilar to engine torque because the vehicle axle torque is influenced by gear selection. Figure 5 shows the average relative contribution of each input to predict NO_x emissions of the vehicles using the 20-input ANNs. It should be noted that ANNs were capable of finding patterns among variables when none of the variables themselves was highly correlated to the outputs. In addition, while two inputs were only slightly correlated, a part of the effect of an input on the output could be assigned to another input. Therefore, the value of a contribution factor should not be considered as an absolute indication of the effect of an input on the output and to decide whether to include a variable in a network.

7 NEURAL NETWORK RESULTS AND DISCUSSION

Based on the association of the vehicle power (separated to hub rotational speed and torque) and emissions, a previous study showed that test schedules with wide speed and torque ranges were able to predict the emissions from the test schedules with similar or lower ranges of speed and torque effectively [**31**]. Therefore among the available test

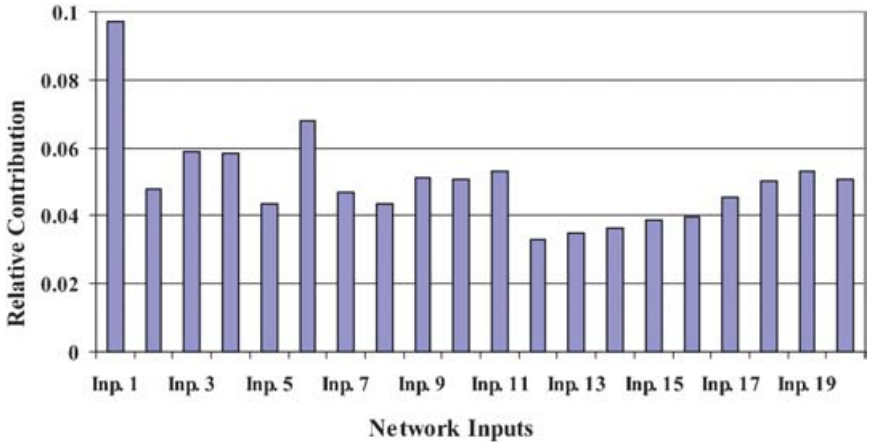

Fig. 5 Average relative contribution of each input to predict NO_x emissions using the 20-input ANN. Table 6 defines the input numbers

schedules, the ANN was trained on the Highway cycle and the trained network was used to predict the CSHVR and UDDS emissions. The ANN was also trained on other test schedules (CSHVR and UDDS) and applied to the remaining cycles for emission prediction, but the ANNs that were trained on the Highway cycle yielded better results, probably because the Highway cycle included both freeway behaviour and acceleration and deceleration sections. These results confirmed the benefit of using the test schedules with a wide range of speed and torque. The network was trained for every vehicle independently and the trained network was applied to the other schedules of the same vehicle, because the ANN cannot project emissions for a different vehicle.

7.1 NO_x prediction results

The 20-input ANN was composed of the dispersed continuous speed and torque data, their first and second derivatives at three different time ranges (1, 5, and 10 seconds), and Diff(t) and Del(t) variables at time ranges of 50, 100, and 150 seconds. The ANN was trained on the Highway cycle. The linear fits of the predicted versus measured NO_x yielded an average R^2 of 0.975 for the six trucks and the best fit had $R^2 = 0.986$. Applying the trained network on other cycles showed an average R^2 of 0.822 (six trucks) and 0.853 (two trucks) for the CSHVR and UDDS respectively. Results are shown in Tables 7, 8, and 9.

A point that interested the researchers was the contribution of the Diff(t) and Del(t) variables and therefore an ANN was trained with only 14 inputs of speed and torque and their first and second derivatives at 1, 5, and 10 seconds. The results are shown in Tables 7 to 9 and compared to the results of the previous method studied at West Virginia University (WVU) [**31**]. The ANN was also trained with 8 inputs including the speed, torque, their first and second derivatives over 1 second, and the Diff(t) and Del(t) variables over the last 150 seconds. The motivation to choose the 150 seconds was due to its contribution to the ANN emissions prediction compared to the 50 and 100 second alternatives. The Diff(t) variable made the fluctuations of the speed smoothed throughout the test schedule. This variable was able to create a steady speed-dependent input for the neural networks. The smoothing conception of the Diff(t) variable also showed that choosing a wider time-frame for this variable can improve the ANN prediction because the emissions were directly relevant to the steady speed. However, if the time-frame was selected to be too wide, it was impossible to follow the rate of the speed change. Therefore, it was very critical to find an appropriate time-frame for this variable. Table 7 shows that the prior WVU study was best in predicting the CSHVR NO_x data, but that the 14-input ANN was close to that in performance. The 20- and 8-input ANNs were worse predictors. The same conclusions were reached for predicting the UDDS NO_x data on two trucks, as shown in Table 9. Interestingly, the 20-input ANN was the best in modelling the Highway cycle when trained on the same cycle, with the 8-input ANN next and the 14-input and prior study last. The predictions using 20 inputs and 8 inputs may have been over-trained on the Highway cycle, and may also have used Diff(t) and Del(t) in a way that did not suit general predictive ability. The 14-input ANN, without these long-term variables, was superior in predicting

Table 7 ANN NO_x emissions prediction results using different numbers of inputs for all six vehicles exercised through the CSHVR. The ANN was trained on the Highway cycle

	20-input	Previous study at WVU [**31**]	14-input	8-input
Vehicle 1*	0.810	0.790	0.811	0.829
Vehicle 2	0.754	0.807	0.825	0.840
Vehicle 3	0.687	0.730	0.732	0.643
Vehicle 4	0.926	0.944	0.933	0.918
Vehicle 5	0.902	0.928	0.907	0.887
Vehicle 6	0.854	0.924	0.888	0.854
Average	0.822	0.853	0.849	0.830

*See Table 1.

Table 8 ANN NO_x emissions prediction results using different numbers of inputs for all six vehicles exercised through the Highway cycle. The ANN was trained on the same cycle

	20-input	Previous study at WVU [**31**]	14-input	8-input
Vehicle 1	0.970	0.971	0.962	0.963
Vehicle 2	0.967	0.937	0.935	0.950
Vehicle 3	0.986	0.971	0.972	0.982
Vehicle 4	0.974	0.952	0.934	0.958
Vehicle 5	0.978	0.939	0.935	0.943
Vehicle 6	0.975	0.870	0.855	0.931
Average	0.975	0.940	0.932	0.955

Table 9 ANN NO_x emissions prediction results using different numbers of inputs for all the vehicles exercised through the UDDS. The ANN was trained on the Highway cycle

	20-input	Previous study at WVU [**31**]	14-input	8-input
Vehicle 1	0.891	0.918	0.918	0.912
Vehicle 2	0.814	0.907	0.900	0.858
Average	0.852	0.912	0.909	0.885

unseen cycles and similar to the performance of the previous [**31**] model. This argument is reflected in the fact that the 20- and 8-input ANNs had specific difficulty in predicting the emissions of truck 3 on the CSHVR; this particular vehicle was identified by the authors to have strong off-cycle behaviour.

Further study of Table 7 shows that no particular ANN was best for all vehicles. The 8-input ANN was best for two, the previous WVU study ANN was best for three, and the 14-input ANN was best for one. The 8-input ANN is attractive in having few variables, opening the argument on accuracy versus ease of use. Figures 6 to 8 show the neural network NO_x prediction for the Highway cycle and the CSHVR for vehicle 1. Figure 7 shows a misprediction of idle emissions at the beginning of the CSHVR, but Fig. 8 shows that the difference between measured and predicted NO_x persisted at all NO_x levels and that there is no noteworthy or systematic pattern to the predictive error.

7.2 CO_2 prediction results

The same ANN architectures were applied to the data to predict CO_2 emissions, as shown in Tables 10 to 12. The average prediction accuracy of the 20-input ANN trained on the Highway cycle was over 0.992 for all six trucks. This ANN was used to predict CO_2 emissions of the other two test schedules. The prediction results (Tables 10 and 12) showed an average

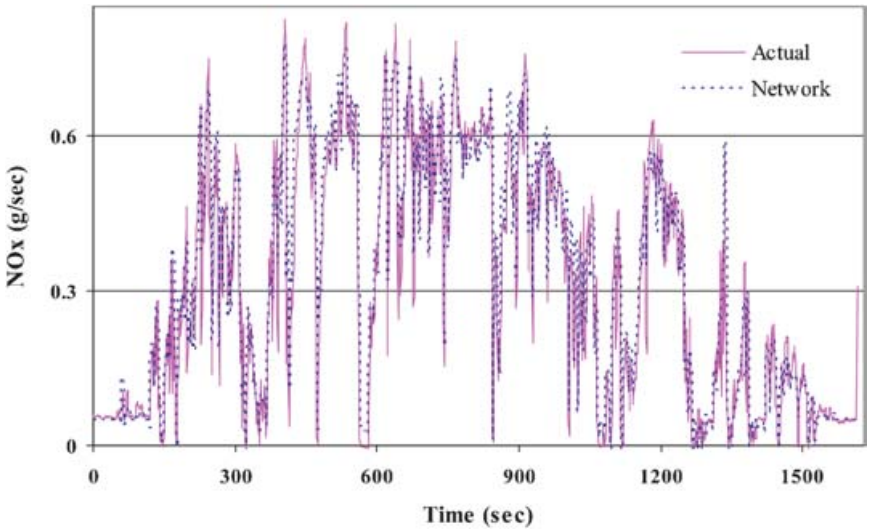

Fig. 6 Actual and ANN prediction of NO_x emissions using 8 inputs for vehicle 1 exercised through the Highway cycle. The ANN was trained on the same cycle

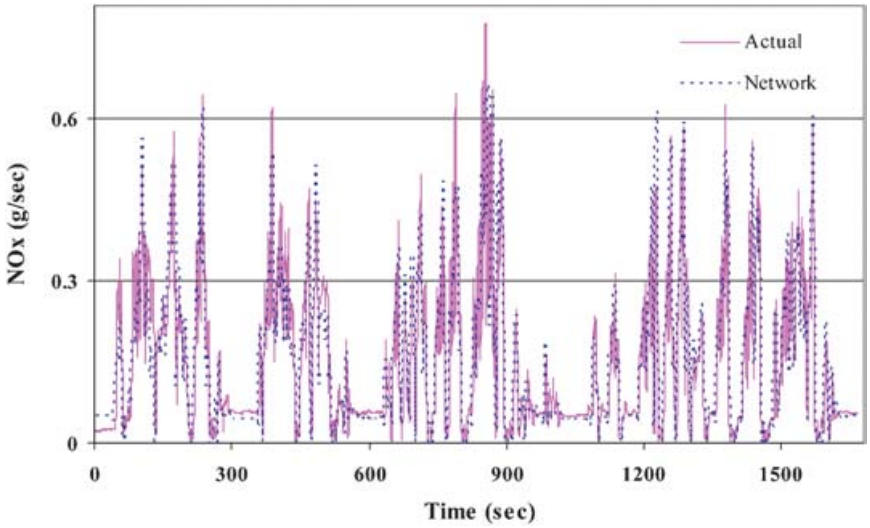

Fig. 7 Actual and ANN prediction of NO_x emissions using 8 inputs for vehicle 1 exercised through the CSHVR. The ANN was trained on the Highway cycle

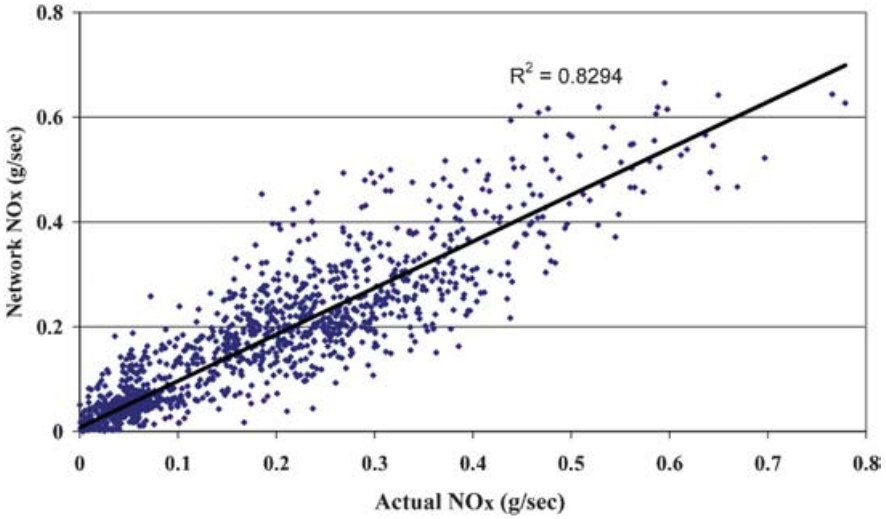

Fig. 8 ANN prediction versus actual NO_x emissions (related to Fig. 7) shows a linear fit of $R^2 = 0.829$

Table 10 ANN CO_2 emissions prediction results using different numbers of inputs for all six vehicles exercised through the CSHVR. The ANN was trained on the Highway cycle

	20-input	Previous study at WVU [31]	14-input	8-input
Vehicle 1	0.963	0.964	0.971	0.972
Vehicle 2	0.928	0.931	0.928	0.937
Vehicle 3	0.964	0.975	0.971	0.975
Vehicle 4	0.972	0.980	0.978	0.979
Vehicle 5	0.969	0.990	0.971	0.973
Vehicle 6	0.953	0.944	0.943	0.950
Average	0.958	0.963	0.960	0.964

Table 11 ANN CO_2 emissions prediction results using different numbers of inputs for all six vehicles exercised through the Highway cycle

	20-input	Previous study at WVU [31]	14-input	8-input
Vehicle 1	0.993	0.992	0.992	0.991
Vehicle 2	0.993	0.990	0.990	0.988
Vehicle 3	0.994	0.992	0.991	0.993
Vehicle 4	0.994	0.985	0.986	0.989
Vehicle 5	0.994	0.990	0.987	0.990
Vehicle 6	0.992	0.981	0.982	0.986
Average	0.993	0.988	0.988	0.989

Table 12 ANN CO_2 emissions prediction results using different numbers of inputs for the vehicles exercised through the UDDS. The ANN was trained on the Highway cycle

	20-input	Previous study at WVU [31]	14-input	8-input
Vehicle 1	0.973	0.977	0.979	0.978
Vehicle 2	0.940	0.939	0.946	0.939
Average	0.956	0.957	0.962	0.958

R^2 of 0.96 for both the CSHVR and UDDS for the 20-input ANN. Table 10 shows that the 8-input ANN is the most accurate architecture for the CO_2 prediction of the CSHVR and UDDS overall, but the results for all four ANNs were very similar. Therefore, the 8-input ANN is favoured due to its accuracy and simplicity in this case.

Figures 9 and 10 show the measured and predicted CO_2 for vehicle 2 exercised through CSHVR and UDDS test schedules respectively. The ANN was trained on the Highway cycle. Visually, the predictions are excellent.

7.3 HC prediction results

HC results are given in Tables 13 to 15. The 20-input ANN yielded an average R^2 of 0.85 for HC prediction of the Highway cycle, on which it was trained. Applying the trained network on other cycles provided an average R^2 of 0.31 for the CSHVR and R^2 of 0.22 for the UDDS test schedules. This is not surprising because HC emissions from many diesel vehicles

Table 13 ANN HC emissions prediction results using different numbers of inputs for all six vehicles exercised through the CSHVR. The ANN was trained on the Highway cycle

	20-input	Previous study at WVU [31]	14-input	8-input
Vehicle 1	0.175	0.178	0.180	0.151
Vehicle 2	0.089	0.181	0.117	0.194
Vehicle 3	0.083	0.006	0.007	0.008
Vehicle 4	0.395	0.455	0.716	0.429
Vehicle 5	0.459	0.412	0.450	0.420
Vehicle 6	0.681	0.602	0.610	0.647
Average	0.314	0.306	0.347	0.308

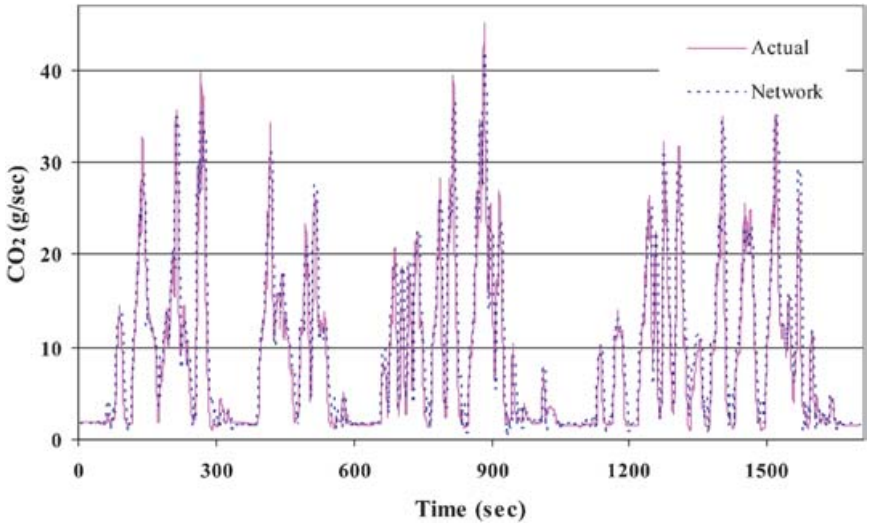

Fig. 9 Actual and ANN prediction of CO_2 emissions using 8 inputs for vehicle 2 exercised through the CSHVR. The ANN was trained on the Highway cycle

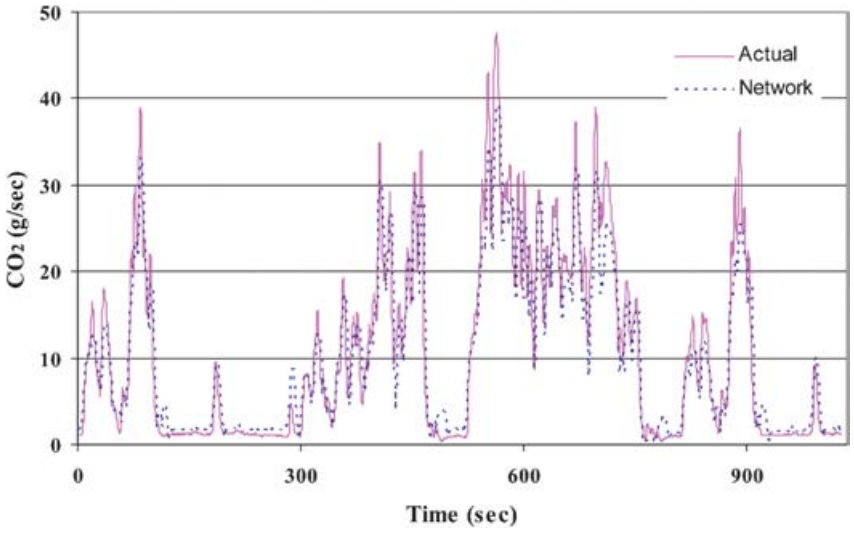

Fig. 10 Actual and ANN prediction of CO_2 emissions using 8 inputs for vehicle 2 exercised through the UDDS. The ANN was trained on the Highway cycle

Table 14 ANN HC emissions prediction results using different numbers of inputs for all six vehicles exercised through the Highway cycle. The ANN was trained on the same cycle

	20-input	Previous study at WVU [31]	14-input	8-input
Vehicle 1	0.865	0.734	0.644	0.866
Vehicle 2	0.873	0.311	0.311	0.262
Vehicle 3	0.886	0.382	0.371	0.659
Vehicle 4	0.618	0.335	0.636	0.452
Vehicle 5	0.907	0.612	0.568	0.822
Vehicle 6	0.954	0.829	0.870	0.930
Average	0.850	0.534	0.567	0.665

Table 15 ANN HC emissions prediction results using different numbers of inputs for the vehicles exercised through the UDDS. The ANN was trained on the Highway cycle

	20-input	Previous study at WVU [31]	14-input	8-input
Vehicle 1	0.449	0.445	0.448	0.486
Vehicle 2	0.008	0.311	0.265	0.334
Average	0.228	0.378	0.356	0.410

are so low that they are difficult to measure and to correct for background data. Also, HC emissions tend not to vary closely with power and tend to be sensitive to the operating temperature and transient

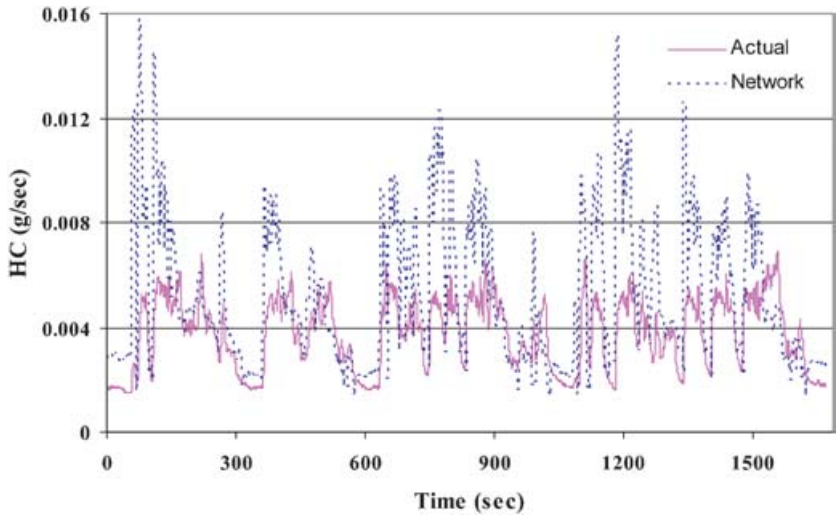

Fig. 11 Actual and ANN prediction of HC emissions using 8 inputs for vehicle 4 exercised through the CSHVR. The ANN was trained on the Highway cycle

behaviour. Figure 11 shows the 8-input ANN prediction of CSHVR HC. The ANN successfully identifies the periods of elevated HC, but underestimates the HC level substantially.

7.4 CO prediction results

Tables 16 to 18 shows the actual versus predicted CO results. CO emissions are strongly dependent on transient events, and high levels of CO arise near full load and during rapid acceleration. As a result, CO emissions are difficult to predict. The 20-input ANN performed well (relative to the other ANN) on the Highway cycle, on which it was trained, but substantially worse in predicting the CSHVR. This is suggestive of overtraining of the 20-input ANN. The ANN trained on 8 inputs was most accurate for the CSHVR prediction, with the highest value for R^2 for five of the six trucks. The 8-input ANN also predicted the CO emissions of the two trucks on the UDDS acceptably. Figure 12 shows that the ANN generally predicted 'spikes' of CO at the appropriate points in the schedule, but that the magnitude of many spikes was poorly modelled. Dispersion effects may contribute to the difficulty in modelling 'spikes' accurately.

For the 8-input ANN, the error between the actual and predicted emissions over each test schedule was calculated and presented in Appendix 4. Positive and negative percentage errors show over- and underprediction respectively.

Table 16 ANN CO emissions prediction results using different numbers of inputs for all six vehicles exercised through the CSHVR. The ANN was trained on the Highway cycle

	20-input	Previous study at WVU [31]	14-input	8-input
Vehicle 1	0.595	0.614	0.603	0.659
Vehicle 2	0.605	0.529	0.541	0.674
Vehicle 3	0.391	0.672	0.662	0.685
Vehicle 4	0.680	0.736	0.780	0.732
Vehicle 5	0.298	0.371	0.313	0.448
Vehicle 6	0.720	0.787	0.796	0.798
Average	0.548	0.618	0.616	0.666

Table 17 ANN CO emissions prediction results using different numbers of inputs for all six vehicles exercised through the Highway cycle. The ANN was trained on the same cycle

	20-input	Previous study at WVU [31]	14-input	8-input
Vehicle 1	0.857	0.779	0.774	0.767
Vehicle 2	0.935	0.795	0.823	0.712
Vehicle 3	0.948	0.678	0.683	0.810
Vehicle 4	0.914	0.710	0.717	0.832
Vehicle 5	0.843	0.615	0.643	0.666
Vehicle 6	0.954	0.844	0.836	0.925
Average	0.908	0.737	0.746	0.785

Table 18 ANN CO emissions prediction results using different numbers of inputs for the vehicles exercised through the UDDS. The ANN was trained on the Highway cycle

	20-input	Previous study at WVU [31]	14-input	8-input
Vehicle 1	0.493	0.591	0.662	0.559
Vehicle 2	0.195	0.302	0.303	0.514
Average	0.344	0.446	0.482	0.536

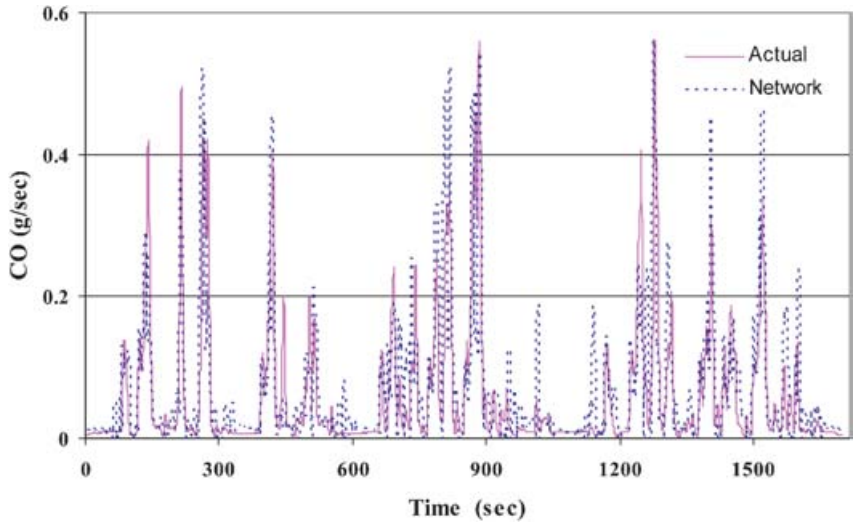

Fig. 12 Actual and ANN prediction of CO emissions using 8 inputs for vehicle 2 exercised through the CSHVR. The ANN was trained on the Highway cycle

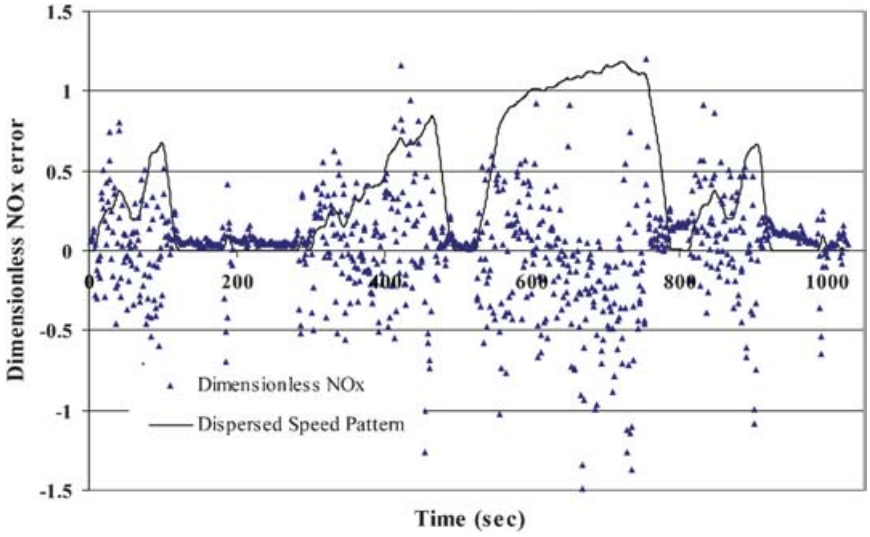

Fig. 13 Difference of ANN predicted and actual real-time NO_x for vehicle 1 exercised through the UDDS. The ANN was trained on the Highway cycle

In each cycle, to investigate the areas of significant difference between the predicted emissions and the measured emissions, the dimensionless difference between predicted and actual values was calculated and plotted against time. Figure 13 shows the difference between predicted and measured NO_x at each second over the UDDS for one vehicle. To compute the dimensionless difference, the difference between the measured and the predicted emissions at each second was divided by the average of the measured emissions. The dispersed speed pattern is illustrated as a solid line in Fig. 13. The predicted NO_x differed more from the actual NO_x when there were sudden changes in the vehicle speed. However, while the speed was constant over periods of the time, the difference was small. NO_x data for the CSHVR showed the same trends. For CO_2, the difference between the actual and predicted emissions followed the speed pattern for the UDDS as well and the rate of speed change was correlated to the magnitude of the predicted and measured emissions differences. The HC and CO prediction differences did not show this trend and were spread with no visual correlation to speed.

8 CONCLUSIONS

ANN modelling proved to be an excellent tool to predict diesel vehicle CO_2 and NO_x emissions.

Among the applied ANN architectures, the one with 8 inputs of axle speed, torque, their first and second derivatives at one second, and novel variables Diff(t) and Del(t), used to examine speed history effects over the last 150 seconds, was the simplest ANN used in the study. Data in this study included 'off-cycle' emissions, which are not generally encountered in test cell engine measurements, and the 8-input ANN included Diff(t) and Del(t) inputs for this purpose. Using training on the Highway cycle, the NO_x prediction on the same cycle was better by the 8-input ANN than the 14-input ANN, but the 20-input ANN was best overall for NO_x on the same cycle. The 20-input model may have been overtrained by the Highway cycle, because it failed to predict the NO_x emissions well for the unseen CSHVR and UDDS cycles. For the case of the CSHVR prediction with Highway cycle training, the 14-input ANN was best, followed by the 8-input ANN and then the 20-input ANN. The 14-input ANN was only marginally superior to the 8-input ANN in prediction, so that the 8-input ANN was considered a better tool when training time was also considered. The same was true for the case of the UDDS prediction with Highway cycle training. For CO_2 prediction, all three ANNs predicted the emissions well, and all three had closer performances than for NO_x. The 14-input and 8-input ANNs were similar, and slightly better than the 20-input ANN for unseen cycle prediction. Overall, the 8-input ANN predicted the CSHVR and UDDS CO emissions better than the other networks when they were trained on the Highway cycle. Though acceptable for the 20-input ANN when it was trained on the same cycle that it predicted, the HC prediction was uniformly poor for all other cases. This is due in part to the low emissions level of HC and difficulty in measuring the concentrations and compensating for background levels. Also, HC is not monotonically related to power as are NO_x and CO_2, so that the correlation with engine behaviour is less clear. The ANN would be well suited to inventory prediction and would allow access to the real-life emissions of a vehicle operated over a roadway route that is very different from the existing tests cycles. How the ANN would be applied to a large fleet with varying emissions has yet to be explored.

ACKNOWLEDGEMENTS

The authors are grateful to WVU field researchers for their acquisition of data in the Gasoline/Diesel PM Split Study and also give special thanks to Ralph Nine for his help in preprocessing the data. The Gasoline/Diesel PM Split Study was supported by the US Department of Energy, Office of Freedom Car and Vehicle Technologies, through the National Renewable Energy Laboratory (NREL), and the role of Dr Douglas Lawson of NREL in that program is acknowledged.

REFERENCES

1 US Environmental Protection Agency, Emission control potential for heavy-duty diesel engines. EPA 420-F-97-015, 1997. http://www.epa.gov/otaq/regs/hd-hwy/f97015.pdf accessed 4/1/2007.
2 **Yanowitz, J., McCormick, R. L.,** and **Graboski, M. S.** In-use emission from heavy-duty diesel vehicle. *Environ. Sci. Technol.*, 2000, **34**(5), 729–740.
3 US Environmental Protection Agency, Technology transfer network clearinghouse for inventories and emission factors – emissions modeling: inventories. http://www.epa.gov/ttn/chief/emch/invent/ accessed 3/31/2007.
4 **Koupal, J., Cumberworth, M., Michaels, H., Beardsley, M.,** and **Brzezinski, D.** Draft design and implementation plan for EPA's multi-scale motor vehicle and equipment emission system (MOVES). EPA 420-P-02-006, 2002. http://www.epa.gov/otaq/models/ngm/p02006.pdf accessed 3/31/2007.
5 **Koupal, J.** Emission rate development. In EPA Office of Transportation and Air Quality, FACA Modeling Workgroup Meeting, 2003. http://www.epa.gov/otaq/models/ngm/mwg1203e.pdf accessed 3/30/2007.
6 **Clark, N. N., Gajendran, P.,** and **Kern, J. M.** A predictive tool for emissions from heavy-duty diesel vehicles. *Environ. Sci. Technol.*, 2003, **37**(1), 7–15.
7 **Clark, N. N., Conley, J., Jarrett, R. P., Nennelli, A.,** and **Toth-Nagy, C.** Emissions modeling of heavy-duty conventional and hybrid electric vehicles. SAE paper 2001-01-3675, 2001.
8 **Krijnsen, H. C., Van Kooten, W. E. J., Calis, H. P. A., Verbeek, R. P.,** and **Vanden Bleek, C. M.** Evaluation of an artificial neural network for NO_x emission prediction from a transient diesel engine as a base for NO_x control. *Can. J. Chem. Engng*, 2000, **78**, 408–417.
9 **Yuanwang, D., Meilin, Z., Dong, X.,** and **Xiaobei, C.** An analysis for effect of cetane number on exhaust emissions from engine with the neural network. *Fuel*, 2002, **81**(15), 1963–1970.
10 **De Lucas, A., Duran, A., Carmona, M.,** and **Lapuerta, M.** Modeling diesel particulate emissions with neural networks. *Fuel*, 2001, **80**(4), 539–548.
11 **Lawson, D. R., Gabele, P., Snow, R., Arnott, W. P., Fujita, E. M., Campbell, D. E., Walker, J. R.,** and **Moosmuller, H.** Analysis of second-by-second gas-phase and PM data from gasoline vehicles in DOE's gasoline/diesel PM split study. In the 14th Coordinating Research Council On-Road Vehicle Emissions Workshop, San Diego, 29–31 March 2004.

12 **Lawson, D. R., Gabele, P., Snow, R., Clark, N., Wayne, W. S., Nine, R. D., Fujita, E. M., Zielinska, B., Arnott, W. P., Campbell, D. E., Walker, J. W., Moosmuller, H., Schauer, J.,** and **Christensen, C.** DOE's Gasoline/Diesel PM Split Study. In the 10th Diesel Engine Emissions Reduction (DEER) Conference, Coronado, California, August–September 2004.

13 **Clark, N. N., Wayne, W. S., Nine, R. D., Buffamonte, T. M., Hall, T., Rapp, B. L., Thompson, G.,** and **Lyons, D. W.** Emissions from diesel-fueled heavy-duty vehicles in Southern California. In SAE/JSAE Spring Fuels and Lubricants Meeting, Yokohama, Japan, 2003, JSAE paper 20030232.

14 California Air Resources Board Chairman's Air Pollution Series. Presentation by D. R. Lawson *et al.* September 2005. http://www.arb.ca.gov/research/seminars/doe/doe.htm accessed 2/28/ 2007.

15 **Lawson, D. R.** and **Gurevich, M.** The DOE/NREL Environmental Science Program. SAE paper 2001-01-2069, 2001.

16 **Clark, N. N., Nine, R. D., Daley J. J.,** and **Atkinson, C. M.** Development of a heavy-duty chassis dynamometer driving route. *Proc. Instn Mech. Engrs, Part D: J. Automobile Engineering*, 1999, **213**(D6), 561–574.

17 **Beychok, M. R.** *Fundamentals of stack gas dispersion*, 3rd edition, 1995 (Milton R. Beychok).

18 **Ramamurthy, R.** and **Clark N. N.** Atmospheric emissions inventory data for heavy duty vehicles. *Environ. Sci. Technol.*, 1999, **33**, 52–62.

19 **Clark, N. N., Jarrett, R. P.,** and **Atkinson, C. M.** Field measurements of particulate matter emissions and exhaust opacity from heavy duty vehicles. *J. Air and Waste Managmt Ass.*, 1999, **49**, 76–84.

20 **Jarrett, R. P.** *Evaluation of opacity, particulate matter, and carbon monoxide from heavy-duty diesel transient chassis tests*. MS Thesis, West Virginia University, Morgantown, West Virginia, 2000.

21 **Baskaran, G.** and **Clark, N. N.** Relationships between instantaneous and measured emissions in heavy duty applications. SAE paper 2001-01-3536, 2001.

22 **Levenspiel, O.** *Chemical reaction engineering*, 3rd edition, 1999 (John Wiley and Sons, Inc., New York).

23 **Nine, R. D., Clark, N. N.,** and **Norton, P.** Effects of multiple driving test schedules performed on two heavy-duty vehicles. *SAE Trans. J. Fuels and Lubricants*, 2001, **109**, 2387–2397.

24 **Pham, D. T.** and **Xing, L.** *Neural networks for identification, prediction and control*, 1995 (Springer-Verlag, London).

25 *MATLAB, neural network toolbox user's guide*, Release 13, 2003 (MathWorks, Inc., Natick, Massachusetts).

26 **Hagan, M. T., Demuth, H. B.,** and **Beale, M.** *Neural network design*, 1996 (PWS Publishing Company, Boston, Massachusetts).

27 *NeuroShell2 user's manual*, 1996 (Ward Systems Group, Inc., Fredrick, Maryland).

28 **Kern, J., Clark, N. N., Nine, R.,** and **Atkinson, C. M.** Factors affecting heavy-duty diesel vehicle emissions. *J. Air and Waste Managmt Ass.*, 2002, **52**, 84–94.

29 **Brodrick, C. J., Dwyer, H. A., Farshchi, M., Harris, D. B.,** and **King, F. G.** Effects of engine speed and accessory load on idling emissions from heavy-duty diesel truck engines. *J. Air and Waste Managmt Assoc.*, 2002, **52**(9).

30 Title 13. California Air Resources Board: Notice of Public Hearing to consider amendments to adopt not-to-exceed and Euro III European Stationary Cycle Emission Test Procedures for the 2005 and subsequent model year heavy-duty diesel engines. www.arb.ca.gov/regact/ntetest/notice.pdf, accessed 4/8/2007.

31 **Clark, N. N., Tehranian, T., Jarrett, R. P.,** and **Nine, R. D.** Translation of distance-specific emissions rates between different heavy duty vehicle chassis test schedules. SAE paper 2002-01-1754, 2002.

32 http://www.eso.org/projects/dfs/papers/jitter99/node10.html, accessed 4/6/2007.

33 **Hashemi, N.** *Effects of artificial neural network speed-based inputs on heavy-duty vehicle emissions prediction*. MS Thesis, West Virginia University, Morgantown, West Virginia, 2004.

APPENDIX 1

Notation

$\boldsymbol{b}$	bias vector
$\mathbf{e}$	scalar error
n	network input
$\boldsymbol{p}$	input vector
s^{m}	sensitivity
t	time
$\mathbf{w}$	weight matrix
α	learning rate

APPENDIX 2

Cross-correlation is a standard method of estimating the degree to which two data series are correlated. The cross-correlation product (represented by $\otimes$) of two complicated functions $f(t)$ and $g(t)$ of a real variable t can be identified by several possible functions. The sum of squared differences method can be used when the data series are of the same units [**32**]

$$f \otimes g = \int_{-\infty}^{+\infty} [f(\tau) - g(t-\tau)]^2 \, \mathrm{d}\tau \tag{7}$$

The other method is termed the sum of products

$$f \otimes g = \int_{-\infty}^{+\infty} f(\tau) g(t-\tau) \, \mathrm{d}\tau \tag{8}$$

These methods may be used to align two signals in time when one signal suffers a time offset relative to the other during data logging. The first method describes a measure of difference between the two functions, which is supposed to be minimized to find the best correlating point. However, the second principle uses a quantity that has to be maximized in order to find the target point. The engine power and the engine emissions data series were cross-correlated. In order to use the sum of squared differences method, the power (hp or kW) and emissions continuous data (g/s) must be dimensionless since they are in different units. The power and emissions data were non-dimensionalized by dividing them by their cycle-averaged values. The two methods agreed very well in results and confirmed one another.

APPENDIX 3

The Levenspiel dispersion model is applicable to turbulent flow in pipes and laminar flow in long tubes or channels. The dispersion coefficient, D, represents the spreading process of the flow. The large quantity of D shows rapid spreading in time [**22**]. To characterize the distribution, the centroid of the distribution, $\bar{t}$, must be described

$$\bar{t} = \frac{\int_0^\infty tC\,\mathrm{d}t}{\int_0^\infty C\,\mathrm{d}t} \tag{9}$$

For small quantities of dispersions ($D/(UL) < 0.01$), the spreading curve is symmetric and belongs to a family of Gaussian curves represented by

$$C_i = \frac{1}{2\sqrt{\pi[D/(UL)]}} \exp\left\{\frac{-(1-\theta_i)^2}{4[D/(UL)]}\right\} \tag{10}$$

where θ_i is $t_i/\bar{t}$ and $D/(UL)$ is the vessel dispersion number, a dimensionless group characterizing the spread in the tunnel. U is the average velocity of the fluid in a tunnel of length L. If $D/(UL) > 0.01$ there is a nonsymmetrical curve. Considering the boundary conditions in experimental devices, the following spreading model is suggested for $D/(UL) > 0.01$ [**22**]

$$C_i = \frac{1}{2\sqrt{\pi\theta_i(D/(UL))}} \exp\left\{\frac{-(1-\theta_i)^2}{4\theta_i[D/(UL)]}\right\} \tag{11}$$

APPENDIX 4

The integration of the actual and ANN predicted emissions over the CSHVR, Highway, and UDDS test schedules is calculated and their percentage errors are presented in Table 19. The 8-input ANN was used to predict the emissions species. Positive and negative percentage errors show over- and underprediction respectively.

Table 19 Percentage errors between the actual and ANN predicted instantaneous NO_x, CO_2, HC, and CO over the CSHVR, Highway, and UDDS test schedules [**33**]

	Emission (%)	Vehicle 1	Vehicle 2	Vehicle 3	Vehicle 4	Vehicle 5	Vehicle 6
CSHVR	NO_x	5.98	20.9	26.9	1.39	9.15	3.33
	CO_2	6.11	−1.04	2.02	−7.73	−1.71	0.09
	HC	35.2	5.31	4.08	−29.1	−3.33	6.20
	CO	0.29	6.28	17.8	−3.87	7.35	−9.46
Highway	NO_x	−0.08	−1.37	−0.09	0.29	0.72	3.59
	CO_2	0.61	−0.45	−0.00	−0.16	−0.07	1.07
	HC	−0.51	4.76	−0.19	3.81	1.06	1.62
	CO	−5.73	−3.31	−4.25	−1.07	−3.17	0.49
UDDS	NO_x	1.13	14.4	—	—	—	—
	CO_2	5.68	10.2	—	—	—	—
	HC	−36.4	6.87	—	—	—	—
	CO	17.3	−12.5	—	—	—	—